

# Dynamic Phase Transition of Black Holes in Massive Gravity

T. K. Safir<sup>\*</sup>

*Department of Physics, National Institute of  
Technology Karnataka, Surathkal 575025, India. and  
Department of Physics, T.K.M College of Arts and Science, Kollam, Kerala 691005, India.*

A. Naveena Kumara<sup>†</sup> and Deepak Vaid<sup>‡</sup>

*Department of Physics, National Institute of  
Technology Karnataka, Surathkal 575025, India.*

Shreyas Punacha<sup>§</sup>

*Department of Oral Health Sciences, School of Dentistry,  
University of Washington, Seattle, WA 98195, USA.*

C. L. Ahmed Rizwan<sup>¶</sup>

*Department of Physics, Government College, Kasaragod, Kerala, 671123, India.*

C. Fairros<sup>\*\*</sup>

*Department of Physics, T.K.M College of Arts and Science, Kollam, Kerala 691005, India.*

## Abstract

The dynamical properties of stable small-large black hole phase transition in dRGT non-linear massive gravity theory are studied based on the underlying free energy landscape. The free energy landscape is constructed by specifying the Gibbs free energy to every state, and the free energy profile is used to study the different black hole phases. The small-large black hole states are characterized by probability distribution functions and the kinetics of phase transition are described by the Fokker-Planck equation. Further, a detailed study of the first passage process is presented which describes the dynamics of phase transitions. Finally, we have investigated the effect of mass and topology on the dynamical properties of phase transitions of black holes in dRGT non-linear massive gravity theory.

PACS numbers:

Keywords: Black hole thermodynamics, Non-linear massive gravity, Free energy landscape, Phase transition

---

\*Electronic address: [stkphy@gmail.com](mailto:stkphy@gmail.com)

†Electronic address: [naviphysics@gmail.com](mailto:naviphysics@gmail.com)

‡Electronic address: [dvoid79@gmail.com](mailto:dvoid79@gmail.com)

§Electronic address: [shreyas4@uw.edu](mailto:shreyas4@uw.edu)

¶Electronic address: [ahmedrizwani@gmail.com](mailto:ahmedrizwani@gmail.com)

\*\*Electronic address: [fairoos.phy@gmail.com](mailto:fairoos.phy@gmail.com)

## I. INTRODUCTION

A black hole is, hopefully, an excellent tool that could be used to unravel the nature of gravity at the quantum mechanical level. The well-established connection between a black hole and an ordinary thermodynamic system [1, 2] has laid a strong foundation for this prospect. Consequently, rigorous studies were conducted to understand gravity from the viewpoint of thermodynamics and statistical physics, and a great deal of advancements have been made in recent years. One of the profound results in this regard is the analogy between the 4-dimensional charged black hole in AdS space and the van der Waal liquid-gas system [3–5]. This formulation was achieved by treating the cosmological constant as thermodynamic pressure and its conjugate quantity as a thermodynamic volume in the extended phase space. Hawking and Page [6] studied the first-order phase transition from a thermal AdS phase to a large black hole phase by considering the black holes as thermodynamic states. Soon the analogy between black holes and van der Waal systems has been explored in modified gravity theories as well as higher curvature gravity theories [7–14]. In thermodynamics, the macroscopic properties of a system can be determined by the microscopic degrees of freedom. In this regard, a phase of a thermodynamics system is a macroscopic emergent state. The probability in which a state emerges from many possible microstates is related to the thermodynamic free energy of the system. The free energy distributed among the state space constitutes a free energy landscape. Further, the free energy landscape can be characterized by specifying an order parameter. In a van der Waal liquid-gas system, the density can be used as an order parameter. The transition between different states, caused by thermal fluctuations, can be addressed in terms of free energy minima.

Black holes, being a thermal entity, can be considered macroscopic emergent states of some underlying microscopic degrees of freedom. Therefore, we can construct a free energy landscape by taking the radius of the black hole as the order parameter [15, 16]. Also, one can study the kinetics of black hole phase transitions using the probabilistic Fokker-Planck equation on the free energy landscape. This formalism has been applied to study the phase transitions in Einstein’s gravity and in massive gravity theories[17]. The calculation can be extended by solving the Fokker-Planck equation subjected to suitable boundary conditions

to obtain the stationary distributions of black hole states at different temperatures as well as the first passage time of the probabilistic evolution between black hole states. Considering this, the dynamics and kinetics of the Hawking-Page phase transition for Reissner-Nordstrom anti-de Sitter (RNAdS) black holes are investigated in [18].

The general theory of relativity is a massless spin two-field theory. One can ask about the possibilities of a self-consistent gravity theory with massive graviton. The answer is yes! Besides, among the several modified gravity theories, massive gravity theories can explain the accelerated expansion of our universe without introducing a cosmological constant or dark energy. Massive gravity theories have a long and remarkable history. The initial studies were carried out by Fierz and Pauli in 1939[19]. The proposed theory was linear and ghost-free but did not reduce to general relativity in the massless limit. Non-linear modifications of Fierz and Pauli’s theory lead to ”Boulware-Deser” ghost instability[20]. Later, de Rham, Gabadadze, and Tolley (dRGT) came up with a special class of non-linear massive gravity theory, which is “Boulware-Deser” ghost free[21]. As mentioned before, the thermodynamics of the black holes in massive gravity were widely investigated [12, 22–27]. The van der Waals-like feature of dRGT massive gravity black holes and other applications such as triple point, Reentrant phase transitions, heat engines, and throttling process were also studied [28–32]. In addition, several works to probe the microstructure were also studied using various thermodynamic-geometry approaches [33–36].

In this paper, we extend the calculation of black hole phase transitions within the free energy landscape by considering a dRGT non-linear massive gravity theory. The free energy landscape is constructed by specifying the Gibbs free energy to every state, and the free energy profile is used to study the different black hole phases. A detailed study of the first passage process is presented which describes the dynamics of phase transitions. Finally, we will investigate the effect of mass and topology on the dynamical properties of phase transitions of black holes in dRGT non-linear massive gravity theory.

The organization of the paper is as follows. In section II and III, we present the thermodynamics and phase transition of the dRGT non-linear massive gravity in the free energy landscape. In section IV, we study the Fokker-Planck equation. The numerical solutions are obtained with reflecting boundary conditions. Also, we discuss the numerical results of the first passage time leaking from small black holes to large black hole phases. In section

V, we investigate the effect of mass and topology on the dynamical properties of the stable small-large black hole phase transition in dRGT non-linear massive gravity theory. The results are summarised in section VI with discussions.

## II. THERMODYNAMIC CHARACTERISATION AND PHASE TRANSITION

We start with a brief discussion of the spacetime and thermodynamic structure of a black hole in dRGT non-linear massive gravity theory in four-dimensional AdS space. The action for the Einstein-dRGT gravity coupled to a non-linear electromagnetic field is given by [37],

$$S = \int d^4x \sqrt{-g} \left[ \frac{1}{16\pi} \left[ R + \frac{6}{l^2} + m^2 \sum_{i=1}^4 c_i \mathcal{U}_i(g, f) \right] - \frac{1}{4\pi} F_{\mu\nu} F^{\mu\nu} \right], \quad (1)$$

where  $F_{\mu\nu} = \partial_\mu A_\nu - \partial_\nu A_\mu$  is the electromagnetic field tensor with vector potential  $A_\mu$ ,  $l$  is AdS radius,  $m$  is related to the graviton mass, and  $c_i$  are coupling parameters. Further,  $f_{\mu\nu}$  is a symmetric tensor as reference metric coupled to the space-time metric  $g_{\mu\nu}$ . Graviton interaction terms are represented by symmetric polynomials  $\mathcal{U}_i$ , and are obtained from a  $4 \times 4$  matrix  $\mathcal{K}_\nu^\mu = \sqrt{g^{\mu\alpha} f_{\nu\alpha}}$ , which have the following forms,

$$\mathcal{U}_1 = [\mathcal{K}]$$

$$\mathcal{U}_2 = [\mathcal{K}]^2 - [\mathcal{K}^2]$$

$$\mathcal{U}_3 = [\mathcal{K}]^3 - 3[\mathcal{K}^2][\mathcal{K}] + 2[\mathcal{K}^3]$$

$$\mathcal{U}_4 = [\mathcal{K}]^4 - 6[\mathcal{K}^2][\mathcal{K}]^2 + 8[\mathcal{K}^3][\mathcal{K}] + 3[\mathcal{K}^2]^2 - 6[\mathcal{K}^4]$$

The solution to the above action for various horizon topologies are given by [22, 38],

$$ds^2 = -f(r)dt^2 + \frac{1}{f(r)}dr^2 + r^2 h_{ij} dx_i dx_j, \quad (2)$$

where  $h_{ij}$  is the metric for two-dimensional hypersurface. The topological parameter ( $k$ ) can take values 0,  $-1$ , or  $1$ , representing planar, hyperbolic, and spherical topology, respectively. With the choice of reference metric  $f_{\mu\nu} = \text{diag}(0, 0, c_0^2 h_{ij})$ , the values of  $\mathcal{U}_i$  becomes  $\mathcal{U}_1 = \frac{2c_0}{r}$ ,  $\mathcal{U}_2 = \frac{2c_0^2}{r^2}$ ,  $\mathcal{U}_3 = \mathcal{U}_4 = 0$ . Now, the metric function reduces to,

$$f(r) = k - \frac{m_0}{r} - \frac{\Lambda r^2}{3} + \frac{q^2}{r^2} + m^2 \left( \frac{c_0 c_1}{2} r + c_0^2 c_2 \right), \quad (3)$$

where integration constants  $m_0$  and  $q$  are related to black hole mass and charge, respectively.  $m$  is the parameter for graviton mass, and in the limiting case of  $m = 0$ , the spacetime reduces to Reissner- Nordstrom black hole solution.

Now, the event horizon ( $r_+$ ) is determined by the largest root of the equation  $f(r) = 0$ . The Hawking temperature of the black hole is related to its surface gravity by the relation  $T_H = \frac{\kappa}{2\pi}$ , where the surface gravity  $\kappa = \frac{1}{2}f'(r_+)$ . As in the case of an asymptotically AdS black hole in four dimensions, one can relate the thermodynamic pressure with cosmological constant [39–41] as,

$$P = -\frac{\Lambda}{8\pi}$$

At this point, the mass, temperature, and entropy of the black hole in Einstein-dRGT gravity coupled to a non-linear electromagnetic field can be expressed in terms of the horizon radius and pressure as follows:

$$\begin{aligned} M &= \left( \frac{r_+}{2} (k + c_0^2 c_2 m^2) + \frac{c_0 c_1 m^2 r_+}{2} + \frac{8}{3} \pi P r_+^2 + \frac{q^2}{4r_+^2} \right), \\ T_H &= \left( 2P r_+ + \frac{k + c_0^2 c_2 m^2}{4\pi r_+} - \frac{q^2}{16\pi r_+^3} + \frac{c_0 c_1 m^2}{4\pi} \right), \\ S &= \pi r_+^2. \end{aligned}$$

The first law of black hole mechanics can be readily written using the above quantities. Further, thermodynamic volume is obtained as,

$$V = \frac{4}{3} \pi r_+^3 = \frac{\pi}{6} v^3, \quad (4)$$

where  $v = 2r_+$  is the specific volume. The equation of state of the system  $P = P(T_H, v)$  is,

$$P = \frac{q^2}{2\pi v^4} - \frac{k + c_0^2 c_2 m^2}{2\pi v^2} + \frac{T_H}{v} - \frac{c_0 c_1 m^2}{4\pi v}. \quad (5)$$

This expression indicates that the black hole exhibits a vdW fluid-like behavior. The critical points for the first order phase-transition between a large black hole phase (LBH) and a small black hole phase (SBH) in the extended phase space can be derived from the conditions,

$$\left( \frac{\partial P}{\partial v} \right)_{T_H=0}, \quad \text{and} \quad \left( \frac{\partial^2 P}{\partial v^2} \right)_{T_H} = 0, \quad (6)$$

we obtain,

$$P_c = \frac{(k + m^2 c_2 c_0^2)^2}{24\pi q^2}, \quad (7)$$

Above the critical pressure  $P_c$ , the black hole temperature  $T_H$  is a monotonic function of the black hole radius. Whereas below the critical pressure black hole temperature have

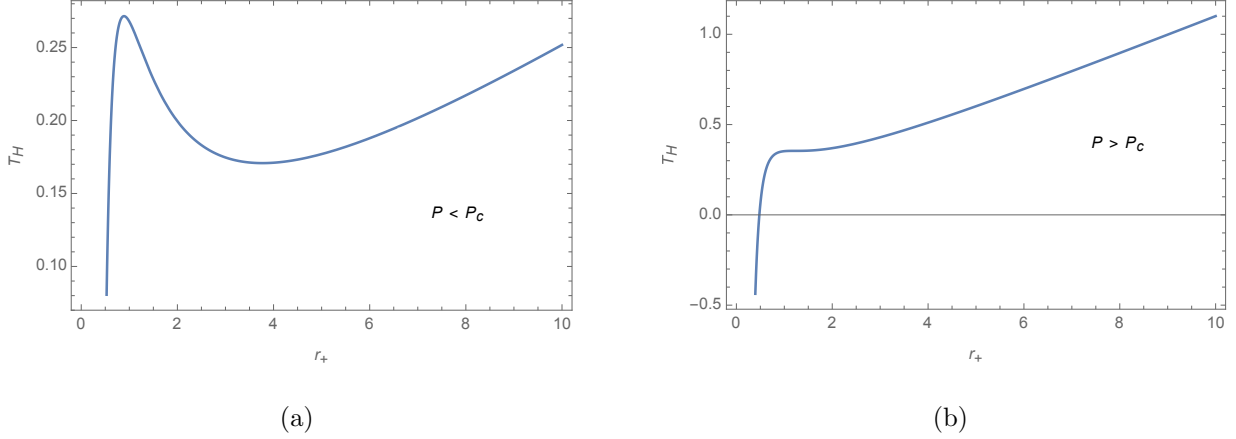


Figure 1: Black hole temperature as a function of event horizon radius (a) when  $P < P_c$  and (b)  $P > P_c$ .

the local minimum and local maximum values (this characteristic is independent of the topology of the system). In Fig. [1] we have depicted a typical behaviour of  $T_H$  as a function of  $r_+$  for both  $P < P_c$  and  $P > P_c$ .

The local minima and local maxima of black hole temperature for  $P < P_c$  are determined by,

$$\frac{\partial T_H}{\partial r_+} = 0,$$

giving the solutions,

$$r_{min/max} = \frac{1}{4\sqrt{\pi}} \left[ \frac{k + c_0^2 m^2 c_2 \mp (k + c_0^2 m^2 c_2 - 24\pi P q^2)^{\frac{1}{2}}}{P} \right]^{\frac{1}{2}}.$$

And the corresponding values of black hole temperatures are given by,

$$T_{min/max} = \frac{1}{4\sqrt{\pi}} \left[ c_0 c_1 m^2 \pi^{\frac{3}{2}} - \frac{16\pi q^2}{\left( \frac{k + c_0^2 m^2 c_2 \mp (k + c_0^2 m^2 c_2 - 24\pi P q^2)^{\frac{1}{2}}}{P} \right)^{\frac{3}{2}}} \right. \\ \left. + \frac{4(k + c_0^2 m^2 c_2)}{\left( \frac{k + c_0^2 m^2 c_2 \mp (k + c_0^2 m^2 c_2 - 24\pi P q^2)^{\frac{1}{2}}}{P} \right)^{\frac{1}{2}}} + 2P \left( \frac{k + c_0^2 m^2 c_2 \mp (k + c_0^2 m^2 c_2 - 24\pi P q^2)^{\frac{1}{2}}}{P} \right)^{\frac{1}{2}} \right]$$

Further analysis shows, when the black hole temperature lies  $T_{min} < T_H < T_{max}$ , there exist three branches of black hole solution (i.e. small, intermediate, and large black hole),

in which the intermediate solution is unstable. Also, there is a first-order phase transition from the small black hole to the large black hole similar to the van der Waals liquid-gas system. The characteristics of the first-order phase transition of the black hole are further studied in the following section using Gibbs free energy landscape.

### III. GIBBS FREE ENERGY LANDSCAPE

We consider a canonical ensemble composed of a series of black hole spacetimes at a given temperature  $T$ . The free energy landscape is constructed by specifying Gibbs free energy to every spacetime state. Now, the Gibbs free energy (on-shell) can be obtained either from the Euclidean action [41] or from the thermodynamic relationship  $G = M - T_H S$ . Note that the expression for off-shell Gibbs free energy is obtained by replacing the Hawking temperature ( $T_H$ ) with the ensemble temperature ( $T$ ), and is given by,

$$G = M - T S = \frac{r_+}{2} \left( k + \frac{q^2}{r_+^2} + \frac{8}{3} P \pi r_+^2 + m^2 \left( c_0^2 c_2 + \frac{c_0 c_1 r_+}{2} \right) \right) - \pi T r_+^2 \quad (8)$$

In this construction, the black hole radius is taken as the order parameter describing the microscopic degrees of freedom of the system. The Gibbs free energy landscape as a function of the black hole radius for  $P < P_c$  at different values of the temperature is studied in Fig. [2]. When  $T < T_{min}$ , there is only one global minimum for the Gibbs free energy and corresponds to the pure radiation phase. At  $T = T_{min}$ , there is an inflection point. Above this temperature, two black hole phases emerge (small and large black hole phases). The smaller and larger black holes correspond to local minima of Gibbs free energy.

For  $T_{min} < T < T_{max}$ , the Gibbs free energy has three local extremals, in which two are stable and one is unstable. The extremum values are determined by,

$$\begin{aligned} \frac{\partial G}{\partial r_+} &= 0 \\ \Rightarrow \frac{k}{2} + \frac{m^2}{2} (c_0^2 c_2 + c_0 c_1 r_+) - \frac{q^2}{2r_+^2} - 2\pi r_+ (T - 2P r_+) &= 0 \end{aligned} \quad (9)$$

Solving this equation for radius, we obtain the radii for small, intermediate, and large black holes. The intermediate black hole which has the maximum value of Gibbs free energy is unstable. The small and large black holes are locally stable as they corresponds to minimal



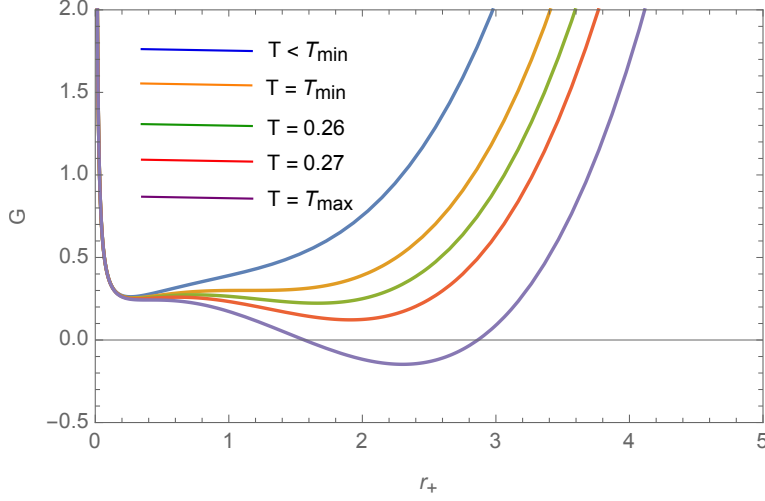


Figure 2: Behaviour of Gibbs free energy as a function of  $r_+$  for  $P < P_c$  at different temperatures

Gibbs free energy. Further, the Gibbs free energy can be obtained as,

$$G_{s/m/l} = \frac{r_{s/m/l}}{2}\eta + \frac{3q^2}{4r_{s/m/l}} - \frac{2}{3}P\pi r_{s/m/l}^3, \quad (10)$$

where  $\eta = k + c_2 m^2$ . One can quantify the free energy landscape topography by constructing free energy barrier heights from the small black hole to the intermediate black hole ( $G(r_m) - G(r_s)$ ) and from the intermediate black hole to the large black hole ( $G(r_m) - G(r_l)$ ). We observe that both barrier heights are monotonic functions of temperature. Similar to the RN-AdS black holes, the barrier height from the small black hole to the intermediate black hole decreases with temperature, whereas, the barrier height from the intermediate black hole to the large black hole increases [18].

As the temperature increases, the local minimum of Gibbs free energy lowers until it becomes zero at  $T = T_{trans}$ , where  $T_{trans}$  is known as the transition temperature. At this point, the Gibbs free energy of large and small black holes are equal. Therefore, the transition temperature can be obtained from the following equations:

$$\begin{aligned} \frac{1}{2}(\eta + c_1 r_s) - \frac{q^2}{2r_s^2} - 2\pi r_s(T - 2Pr_s) &= 0, \\ \frac{1}{2}(\eta + c_1 r_l) - \frac{q^2}{2r_l^2} - 2\pi r_l(T - 2Pr_l) &= 0, \\ \text{and } \frac{r_s}{2}\eta + \frac{3q^2}{4r_s} - \frac{2}{3}P\pi r_s^3 &= \frac{r_l}{2}\eta + \frac{3q^2}{4r_l} - \frac{2}{3}P\pi r_l^3; \end{aligned}$$

The expressions for the small and large black hole radii is readily obtained as,

$$r_s = \frac{1}{8(\pi P)^{\frac{3}{2}}} \left[ (\eta + \omega) (\eta (\eta + \omega) - 12P\pi q^2) \right]^{\frac{1}{2}},$$

$$r_l = \frac{1}{4\pi P(\eta + \omega)} \left[ \eta (\eta + \omega) - 12P\pi q^2 + 4\sqrt{\pi} (P(\eta + \omega) (\eta (\eta + \omega) - 12P\pi q^2))^{\frac{1}{2}} \right]. \quad (11)$$

Here,  $\omega = \sqrt{\eta^2 - 24P\pi q^2}$ . These expressions can be substituted back to obtain the transition temperature.

$$T_{trans} = \frac{6\sqrt{P\pi}t^2(\eta + \omega) - 2q^2(P\pi)^{\frac{3}{2}}(49\eta + 13\omega) + c_1m^2(\eta + \omega)^{\frac{3}{2}}\sqrt{\eta(\eta + \omega) - 12\pi Pq^2}}{2\pi(\eta + \omega)^{\frac{3}{2}}\sqrt{\eta(\eta + \omega) - 12\pi Pq^2}}$$

A thermodynamic phase diagram is given by plotting  $T_{max}$ ,  $T_{min}$ , and  $T_{trans}$  as a function of  $P$ . For a chosen parameters of the system ( $k = 1, m = 1, q = c_1 = c_2 = 0.05$ ), the curves divide the  $P - T$  plane into four thermodynamic phase regions. In Fig. [3], the blue, black, and red lines represent  $T_{max}$ ,  $T_{trans}$ , and  $T_{min}$  respectively.

Note that the structure of the phase diagram is similar to the case of AdS black hole [18].

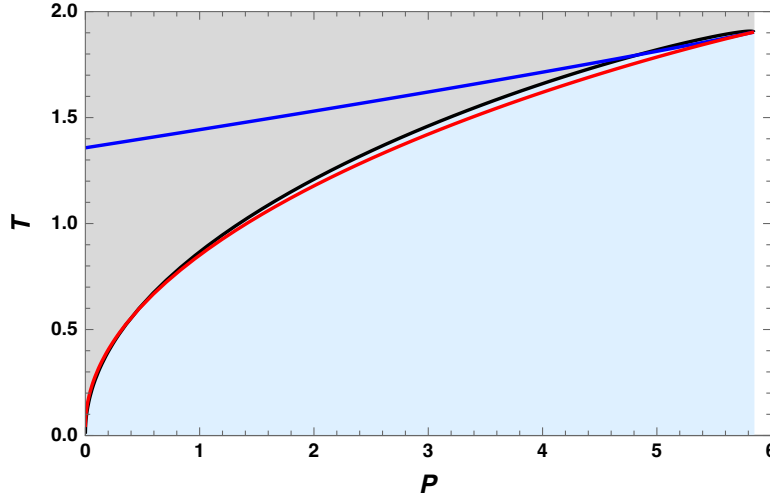


Figure 3: The phase diagram of dRGT black holes. Here,  $T_{max}$ ,  $T_{min}$ , and  $T_{trans}$  are plotted as a function of  $P$  from 0 to  $P_c$ . The small black hole is stable in the blue region whereas the large black hole is stable in the grey region. In this plot, the black line represents the coexisting curve.

The region above the blue line as well as below the red line has only one black hole solution which is always thermodynamically stable. The rest of the phase diagram represents three black hole solutions. Along the black curve, the free energies of small and large black holes are equal, and both these solutions coexist along this curve with equal probability.

Therefore, the black line is called the coexisting curve. We observe that the free energy of the small black hole phase is less than the free energy of the large black hole in the region between the black and red curves, and the free energy of the small black hole phase is greater than the free energy of the larger black hole in the region between the black and blue curves. As the system having less Gibbs free energy is thermodynamically stable, we conclude that the small black hole is stable in the region between the red and black curves whereas the large black hole is thermodynamically stable in the region enclosed by the black and blue lines. However, from the ensemble point of view, one stable black hole state may turn into another stable state due to thermal fluctuations. The dynamics of such evolution of the system are described by the probabilistic Fokker-Planck equation. We will investigate the dynamics of the phase transition in the following section.

#### IV. PROBABILISTIC EVOLUTION ON THE FREE ENERGY LANDSCAPE

In this section, we study the kinetics of black hole phase transition by considering black holes as thermodynamic states in the extended phase space. We have observed that the large and small black hole phases can switch into each other due to the presence of thermal fluctuations. Note that the black hole radius  $r_+$  is taken as the order parameter which characterizes the black hole phases. Therefore, the probability distribution of the thermodynamic state can be considered as a function of  $r_+$  and time  $t$ .

##### A. Fokker-Planck equation and probabilistic evolution

We denote the distribution function  $\rho(r_+, t)$ . Now, the evolution of the distribution is governed by the probabilistic Fokker-Planck equation given by

$$\frac{\partial \rho(r_+, t)}{\partial t} = D \frac{\partial}{\partial r} \left\{ e^{-\beta G(r_+)} \frac{\partial}{\partial r} \left[ e^{\beta G(r_+)} \rho(r_+, t) \right] \right\} \quad (12)$$

Here,  $D$  is the diffusion coefficient and is given by  $D = kT/\xi$ , with  $k$ ,  $\xi$  denoting the Boltzmann constant and dissipation coefficient respectively. Also, the quantity  $\beta = 1/(kT)$  is the inverse temperature of the system. For convenience, we take  $k = \xi = 1$  without the loss of generality.

To solve the Fokker-Planck equation, we need to impose two boundary conditions. The first one is the reflecting boundary condition which preserves the normalization of the probability distribution. At  $r_+ = r_0$ , we set,

$$e^{-\beta G(r_+)} \frac{\partial}{\partial r} [e^{\beta G(r_+)} \rho(r_+, t)] \Big|_{r_+=r_0} = 0,$$

which can be rewritten as,

$$\beta G'(r_+) \rho(r_+, t) + \rho'(r_+, t) \Big|_{r_+=r_0} = 0, \quad (13)$$

where the prime denotes the derivative with respect to the order parameter  $r_+$ . The second boundary condition sets the value of the distribution function to zero,

$$\rho(r_0, t) = 0 \quad (14)$$

In the following analysis, we chose the reflecting boundary condition at  $r_0 = 0$  and  $r_0 = \infty$ . The initial distribution is taken to be a Gaussian wave packet located at  $r_i$ , which is a good approximation of  $\delta$ - distribution.

$$\rho(r_+, 0) = \frac{1}{\sqrt{\pi}a} e^{-\frac{(r-r_i)^2}{a^2}}, \quad (15)$$

where the parameter  $a$  is a constant that determines the initial width of the wave packet. Note that the initial distribution is well normalized, and as a consequence of the reflection boundary condition,  $\rho(r_+, t)$  will remain normalized during the evolution. The parameter  $r_i$  denotes the radius of the initial black hole state. We may choose either  $r_i = r_s$  representing SBH as the initial state or  $r_i = r_l$  for LBH. Suppose we chose  $r_i = r_l$  at  $t = 0$ . As the distribution evolves, we observe a non-zero probability distribution for both SBH and LBH states. This indicates the phase transition between LBH and SBH phases due to thermal fluctuations. The time evolution of  $\rho(r_+, t)$  is plotted in Fig. (4).

In Fig. 4(a) and 4(b), we set  $r_i = r_s$ , and studied the evolution of the distribution for two values of the transition temperatures ( $T_{trans} = 0.4, 0.5$ ). Initially, the probabilistic distribution is peaked at  $r_+ = r_s$ . The probabilistic distribution becomes quasi-stationary in a short time with peaks at small and large black hole states. After some time, the height of  $\rho(r_+, t)$  at  $r_+ = r_s$  decreases while another peak starts to develop at  $r_+ = r_l$ . This implies the leakage of small black hole state to large black hole state. Further, as  $t \rightarrow \infty$ ,  $\rho(r_+, t)$

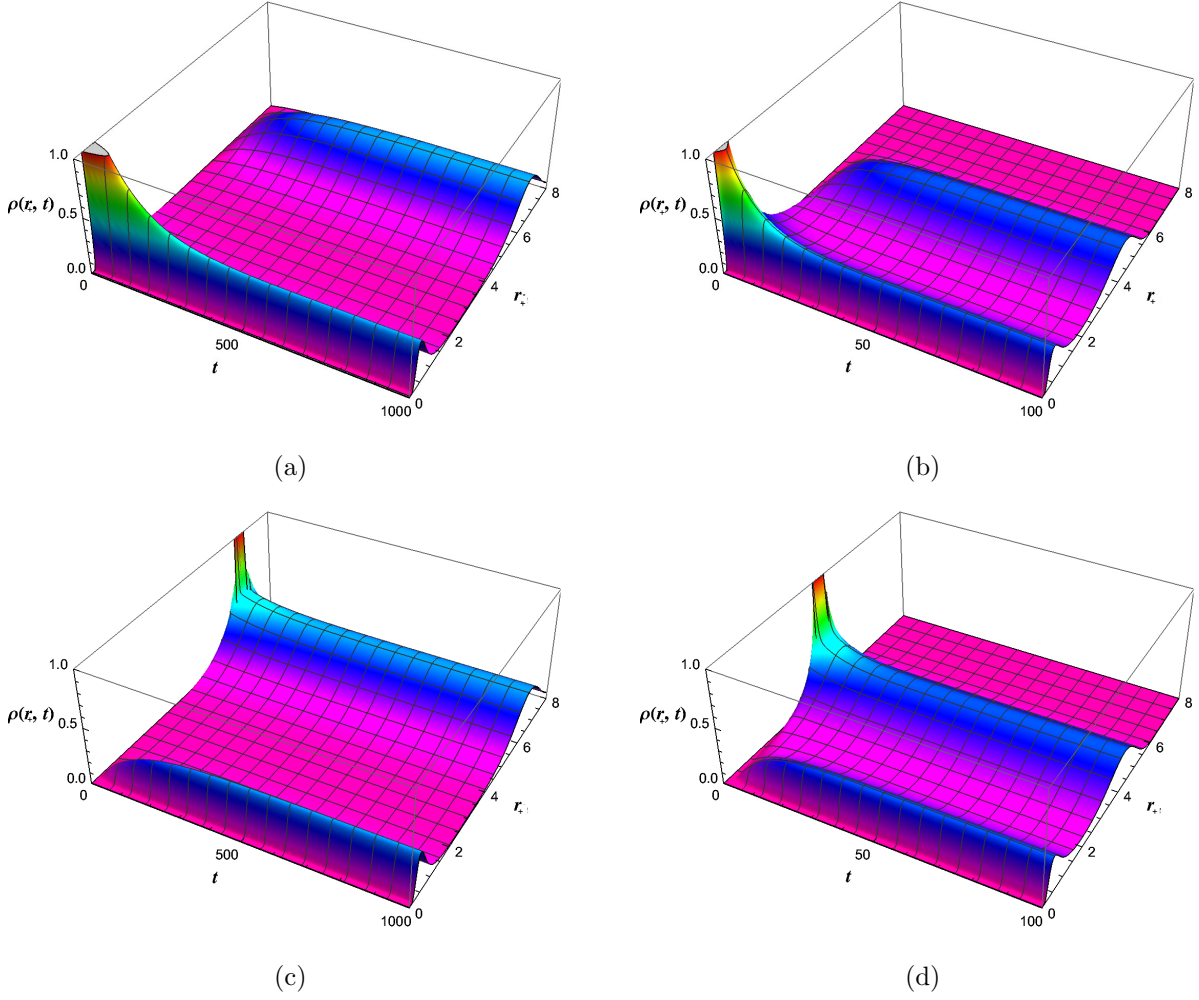


Figure 4: The time evolution of the probability distribution function  $\rho(r_+, t)$ . In (a) and (b) the initial condition is chosen at SBH state and in (c) and (d) it is at LBH state. The reflecting boundary conditions are imposed at  $r = 0$  and  $r = \infty$ . The coexistent temperatures are  $T_{trans} = 0.4$  in left panel) and  $T_{trans} = 0.5$  in right panel) with  $c_1 = 2, q = 1, m = 1, c_0 = 1, c_2 = 5$  and  $k = 1$ .

becomes a stationary state. A similar behavior is observed if we take the initial state to be a large black hole. The corresponding evolution for two different temperatures is depicted in Fig. 4(c), and 4(d).

The above analysis can be made more apparent by comparing the behavior of  $\rho(r_s, t)$  and  $\rho(r_l, t)$  as time progresses, where  $\rho(r_s, t)$ ,  $\rho(r_l, t)$  represent the probability distribution of SBH and LBH states respectively. In Fig. 5, the evolution of probability distribution for both black hole states is depicted for two different transition temperatures. In both

cases, we have taken the initial black hole state to be SBH. In other words, at  $t = 0$ ,  $\rho(r_s)$  takes a finite value but  $\rho(r_l)$  vanishes. Fig. 5(a) describes the evolution of both probability distributions for a transition temperature  $T_{trans} = 0.4$ . Now, as time increases, the height of  $\rho(r_s, t)$  decreases while that of  $\rho(r_l, t)$  increases, indicating the leakage of black hole states from SBH to LBH. For large values of time, both  $\rho(r_s, t)$  and  $\rho(r_l, t)$  approaches a final stationary state where  $\rho(r_s) = \rho(r_l)$ . In Fig. 5(b), the same evolution is drawn but for a higher transition temperature,  $T_{trans} = 0.5$ . From the figure, we observe that for larger transition temperatures, both distributions reach the stationary state more rapidly. A similar analysis can be carried out by taking other black hole states as the initial configuration giving the same results.

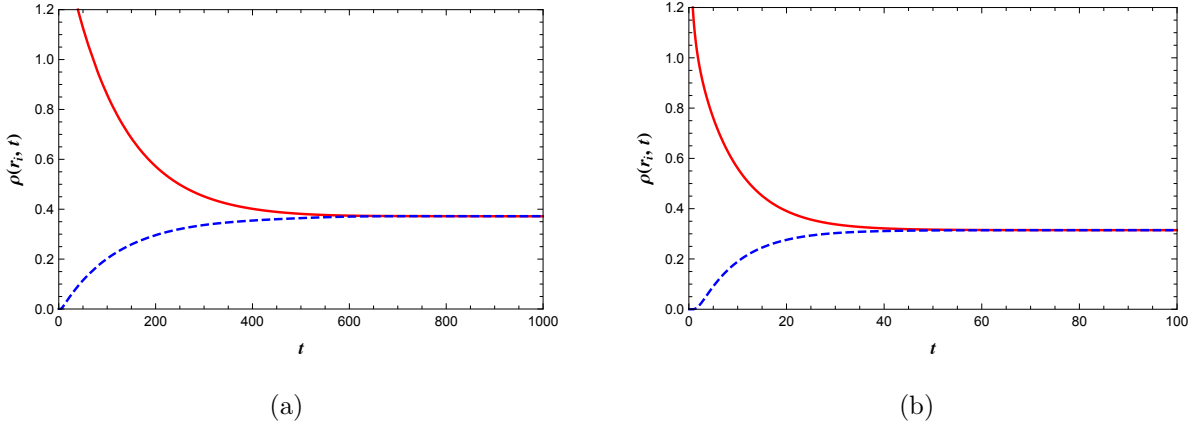


Figure 5: The time evolution of the probability distribution  $\rho(r_+, t)$ . The solid red and dashed blue curves correspond to the functions  $\rho(r_s, t)$  and  $\rho(r_l, t)$ , respectively. The initial Gaussian wave packet is located at SBH state. The coexistent temperatures are (a)  $T_{trans} = 0.4$ . (b)  $T_{trans} = 0.5$ , with  $c_1 = 2, q = 1, m = 1, c_0 = 1, c_2 = 5$  and  $k = 1$ .

In the coming session, we discuss the kinetics by first passage process from one black hole state to another black hole state on the underlying free energy landscape. First passage time is a very important quantity in transition state theory, as the mean first passage time defines an average timescale for a stochastic event to occur first.

## B. First passage time

The first passage time is defined as the time required for the state of a black hole from a stable phase (described by the minimum of Gibbs free energy) to reach the intermediate transition state (described by the maximum of Gibbs free energy) for the first time. Note that the black hole phase transition between the two states under consideration is due to the thermal fluctuations in the system. Therefore, the first passage time will be a random variable. The probability that the present state of SBH that has not made a first passage by time  $t$  is defined as,

$$\Sigma(t) = \int_0^{r_m} \rho(r_+, t) dr_+, \quad (16)$$

where  $r_m$  is the radius of the intermediate black hole state obtained from Eq. (9). As time progress, the probability that the system remains at SBH decreases and approaches zero as  $t \rightarrow \infty$ , i.e.,  $\Sigma(t)_{t \rightarrow \infty} = 0$ . This is due to the fact that the normalization of the probability distribution is preserved in this case. Similarly, one can start with an LBH state and define the probability distribution that the initial LBH state has not made a first passage by time  $t$  as,

$$\Sigma(t) = \int_{r_m}^{\infty} \rho(r_+, t) dr_+, \quad (17)$$

The time evolution of  $\Sigma(t)$  for both SBH and LBH for two values of transition temperatures are plotted in Fig. 6. The probability distribution is clearly seen to vanish for long-time evolutions. Further, the probability distribution decreases faster for transitions at higher temperatures.

Now, the first passage time is the probability that a small black hole state passes through the intermediate state for the first time in the interval  $(t, t + dt)$ . The distribution of first passage time is given by,

$$F_p(t) = -\frac{d\Sigma(t)}{dt} \quad (18)$$

Substituting for  $\Sigma(t)$  and using the Fokker-Planck's equation along with the reflecting boundary condition at  $r_+ = 0$  and absorbing boundary condition at  $r_+ = r_m$ , we get the following expression for the first passage time.

$$F_p(t) = -D \frac{\partial}{\partial t} \rho(r_+, t) \Big|_{r=r_m} \quad (19)$$

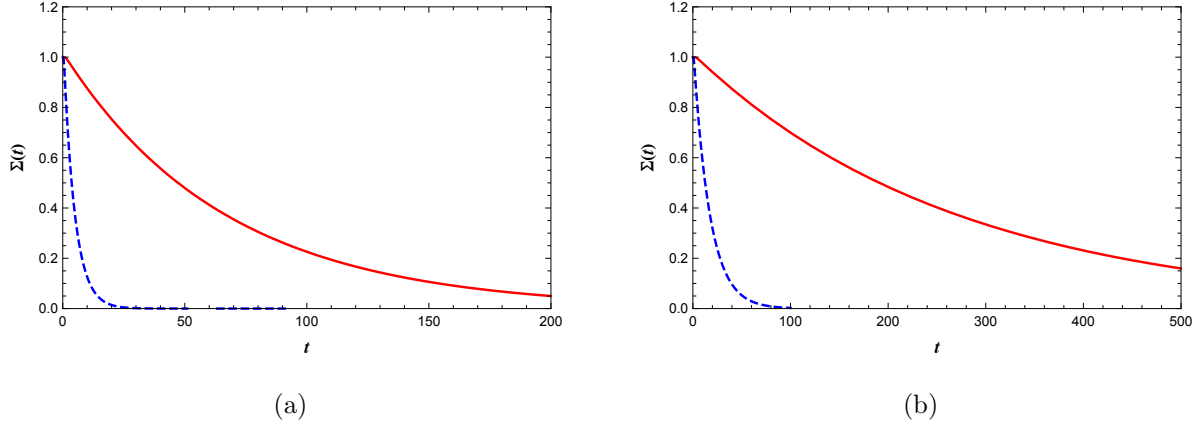


Figure 6: The time evolution of the distribution of the probability  $\Sigma(t)$  that the system remains at the initial state. (a) Initially at SBH and (b) initially at LBH state. Red solid and blue dashed curves are for the coexistent temperatures  $T_{trans} = 0.4$  and  $T_{trans} = 0.5$ , respectively, with  $c_1 = 2, q = 1, m = 1, c_0 = 1, c_2 = 5$  and  $k = 1$ .

The distribution of first passage time for both SBH to LBH and LBH to SBH phase transitions are plotted for different transition temperatures (Fig. 7). In Fig. 7(a), the initial distributions are Gaussian wave packets located at the small black hole state. The single peak in the first passage time within a short period of time indicates that a considerable fraction of the first passage events have occurred before the distribution attains its exponential decay form. As time increases the peak becomes more sharper. The curves corresponding to different transition temperatures show similar behavior of the first passage time. Further, when the initial state is SBH, the location of the peak moves to the left (lower value of time) when the transition occurs at larger transition temperatures. These characteristics can be justified by looking at the behavior of the barrier height between the small and intermediate black hole states as a function of temperature. As mentioned in III,  $G(r_m) - G(r_s)$  decreases as temperature increases. Therefore, the small black hole state can cross the barrier to reach the intermediate state easily at higher transition temperatures. However, if the initial distribution is peaked at a large black hole state, the location of the peak moves to the right (higher values of time) when the transition occurs at larger transition temperatures Fig. 7(b). Similar to the previous case, this behavior is explained as follows: As the barrier height  $G(r_m) - G(r_l)$  increases with the temperature, the large black hole state takes more time to cross the barrier under thermal fluctuations. These results are qualitatively similar



to the case of dynamics of phase transitions charged AdS black holes presented in [18].

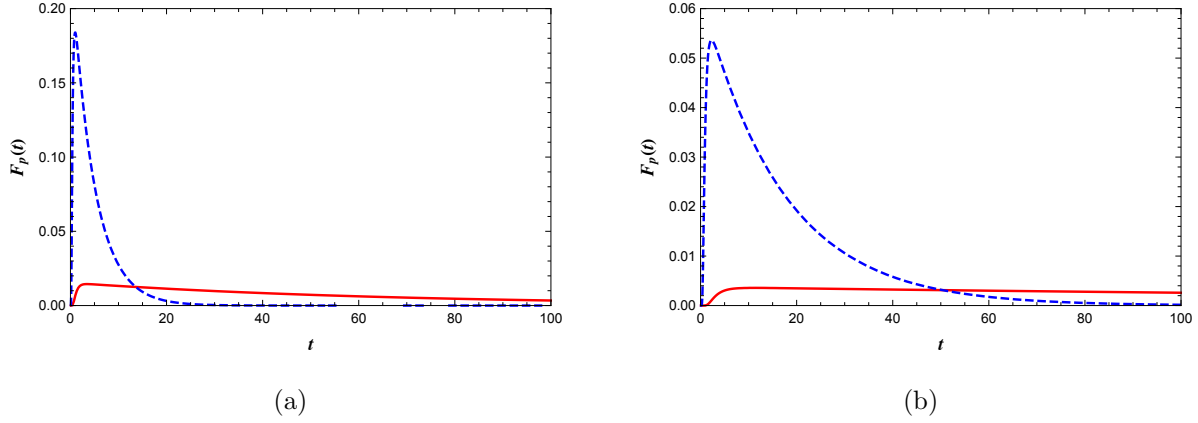


Figure 7: The probability distribution of the first passage time  $F_p(t)$ . Red solid and blue dashed curves are for the coexistent temperatures  $T_{trans} = 0.4$  and  $T_{trans} = 0.5$ , respectively. (a) From SBH state to LBH state. (b) From LBH state to SBH state. Here,  $c_1 = 2, q = 1, m = 1, c_0 = 1, c_2 = 5$  and  $k = 1$ .

In the following, we investigate the role of mass and the topological parameter on the results discussed above on the dynamic phase transition of black holes in massive gravity theory.

## V. THE EFFECT OF MASS AND TOPOLOGY

Note that the numerical results presented so far in the investigation of the dynamics of black hole phase transition in dRGT non-linear massive gravity theory consider only certain values of the parameters in the system. It remains to study the behavior of time evolution of the probability distribution and the first passage time by varying those parameters. However, as the theory possess too many variables, we will be considering the effect of mass and topology only.

In Fig. 8, the evolution of the probability distribution function is plotted for different topologies and masses. Here, we have considered planar ( $\kappa = 0$ ), hyperbolic ( $\kappa = -1$ ), and spherical ( $\kappa = 1$ ) topologies. For the sake of demonstration, the initial black hole is taken as the small black hole (SBH) state and the transition temperature is  $T_{trans} = 0.4$  (Fig. 8(a)). One can see from the figure that the height of  $\rho(r_s, t)$  decreases rapidly for

$\kappa = -1$ , indicating a quick leakage of the black hole state from SBH to LBH. In the case of planar topology, the transition is less rapid and in the spherical case, the evolution is slow. This means that out of three, the spherical black holes attain the stationary state only after a long evolution. Further, the value of the probability distribution at the stationary state ( $\rho(r_s) = \rho(r_l)$ ) is highest for the spherical case compared to the planar and hyperbolic cases. The effect of the mass parameter shows similar behavior. As  $m$  increases, the system attains its final stationary state slowly, i.e., as the mass increases the small black hole state leaks towards the large black hole state slowly (Fig 8(b)).

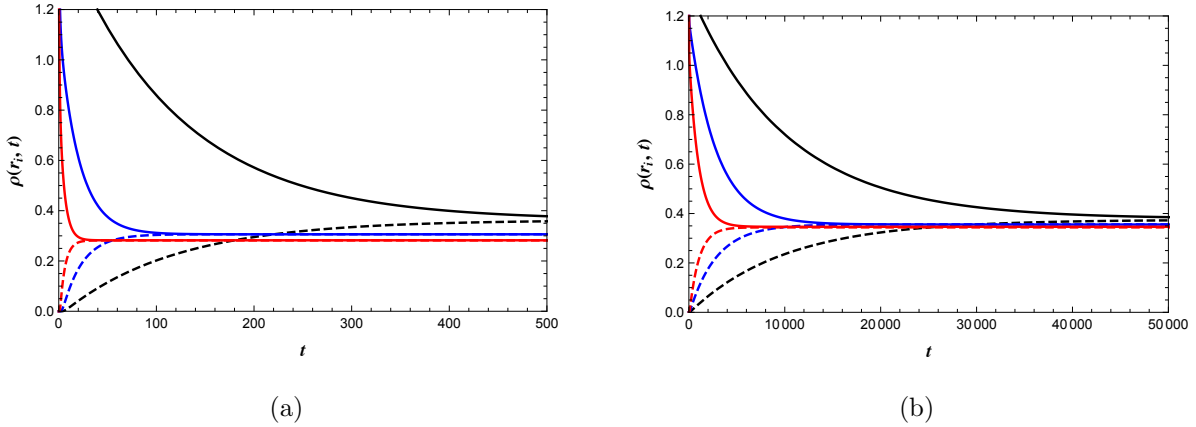


Figure 8: The effect of the parameters on the time evolution of the probability distribution  $\rho(r_+, t)$ . The solid and dashed curves correspond to the functions  $\rho(r_s, t)$  and  $\rho(r_l, t)$ , respectively. The initial Gaussian wave packet is located at SBH state. (a) The effect of topology. Black, blue and red correspond to  $k = 1, 0, -1$ , respectively. The coexistent temperature is  $T_{trans} = 0.4$ . (b) The effect of mass parameter  $m$ . Red, blue and black correspond to  $m = 0, 0.07, 0.1$ , respectively. The coexistent temperature is  $T_{trans} = 0.03$ . The other parameters in these two plots are,  $c_1 = 2, q = 1, m = 1, c_0 = 1, c_2 = 5$  and  $k = 1$ .

Next, we address the effect of topology and mass on the probability distribution of first passage time. In Fig. 9., we have considered an initial small black hole state with the topologies  $\kappa = 0, -1$  and 1. For a given transition temperature, the small black hole state reaches the intermediate state in a small duration of time for hyperbolic topology. In the case of spherical topology, the corresponding time is maximum Fig. 9(a). Further, we observe that the time taken to reach the intermediate state, starting from a SBH increases as mass

increases (Fig. 9(b)).

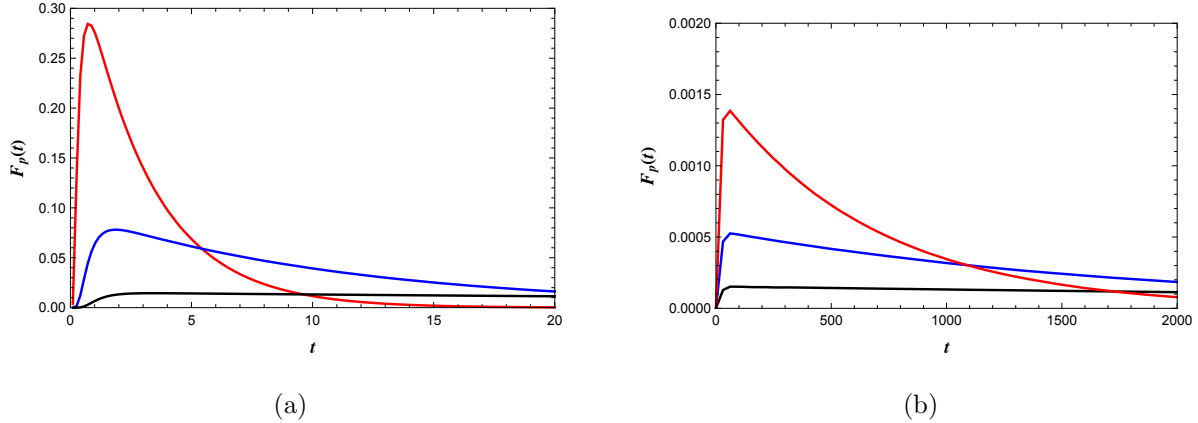


Figure 9: The effect of the spacetime parameters on the probability distribution of the first passage time  $F_p(t)$ . We consider the case for SBH (initial) state to LBH state. (a) The effect of topology. Black, blue and red solid lines are for  $k = 1, 0, -1$ , respectively. The coexistent temperature is  $T_{trans} = 0.4$ . (b) The effect of mass parameter  $m$ . Red, blue and black correspond to  $m = 0, 0.07, 0.1$ , respectively. The coexistent temperature is  $T_{trans} = 0.03$ . The other parameters in these two plots are,  $c_1 = 2, q = 1, m = 1, c_0 = 1, c_2 = 5$  and  $k = 1$ .

## VI. DISCUSSIONS

In this paper, we have studied the dynamics of black hole phase transitions in dRGT non-linear massive gravity theory using the free energy landscape. Thermodynamic characterization and different black hole phases are discussed by considering the black hole radius as the order parameter. Emergent phases of small and large black holes as well as the co-existing curve between these states are shown. The switching of one black hole phase to another due to thermal fluctuations are addressed in terms of first passage time. Further, we have solved the Fokker-Planck equation numerically and the results are explained. The results we have presented are qualitatively similar to the findings of [18]. Finally, we have discussed the effect of mass parameters and the topology on the evolution of black hole phase transition between small and large black hole states. We believe that the variation of switching time from small black holes to large black hole states with respect to the mass as well as the topology is connected to the stability of black holes and will be addressed in future works. Also, we would like to revisit the properties of black hole phase transitions by

incorporating Hawking radiation.

## Acknowledgments

TKS thanks Aparna L. R. for the support and suggestions.

- 
- [1] S. W. Hawking, *Particle Creation by Black Holes*, *Commun. Math. Phys.* **43** (1975) 199.
  - [2] J. D. Bekenstein, *Black holes and entropy*, *Phys. Rev.* **D7** (1973) 2333.
  - [3] D. Kubiznak and R. B. Mann, *P-V criticality of charged AdS black holes*, *JHEP* **07** (2012) 033 [[1205.0559](#)].
  - [4] S. Gunasekaran, R. B. Mann and D. Kubiznak, *Extended phase space thermodynamics for charged and rotating black holes and Born-Infeld vacuum polarization*, *JHEP* **11** (2012) 110 [[1208.6251](#)].
  - [5] D. Kubiznak, R. B. Mann and M. Teo, *Black hole chemistry: thermodynamics with Lambda*, *Class. Quant. Grav.* **34** (2017) 063001 [[1608.06147](#)].
  - [6] S. W. Hawking and D. N. Page, *Thermodynamics of Black Holes in anti-De Sitter Space*, *Commun. Math. Phys.* **87** (1983) 577.
  - [7] R.-G. Cai, L.-M. Cao, L. Li and R.-Q. Yang, *P-V criticality in the extended phase space of Gauss-Bonnet black holes in AdS space*, *JHEP* **09** (2013) 005 [[1306.6233](#)].
  - [8] S.-W. Wei and Y.-X. Liu, *Critical phenomena and thermodynamic geometry of charged gauss-bonnet ads black holes*, *Phys. Rev. D* **87** (2013) 044014.
  - [9] D.-C. Zou, S.-J. Zhang and B. Wang, *Critical behavior of born-infeld ads black holes in the extended phase space thermodynamics*, *Phys. Rev. D* **89** (2014) 044002.
  - [10] A. Rajagopal, D. Kubizňák and R. B. Mann, *Van der Waals black hole*, *Phys. Lett. B* **737** (2014) 277 [[1408.1105](#)].
  - [11] J.-X. Mo and W.-B. Liu, *P – V criticality of topological black holes in Lovelock-Born-Infeld gravity*, *Eur. Phys. J. C* **74** (2014) 2836 [[1401.0785](#)].
  - [12] J. Xu, L.-M. Cao and Y.-P. Hu, *P-V criticality in the extended phase space of black holes in massive gravity*, *Phys. Rev. D* **91** (2015) 124033 [[1506.03578](#)].

- [13] H. Yazdikarimi, A. Sheykhi and Z. Dayyani, *Critical behavior of gauss-bonnet black holes via an alternative phase space*, *Phys. Rev. D* **99** (2019) 124017.
- [14] Z. Dayyani, A. Sheykhi, M. H. Dehghani and S. Hajkhalili, *Critical behavior and phase transition of dilaton black holes with nonlinear electrodynamics*, *Eur. Phys. J. C* **78** (2018) 152 [[1709.06875](#)].
- [15] S.-W. Wei and Y.-X. Liu, *Insight into the Microscopic Structure of an AdS Black Hole from a Thermodynamical Phase Transition*, *Phys. Rev. Lett.* **115** (2015) 111302 [[1502.00386](#)].
- [16] S.-W. Wei, Y.-X. Liu and R. B. Mann, *Repulsive Interactions and Universal Properties of Charged Anti-de Sitter Black Hole Microstructures*, *Phys. Rev. Lett.* **123** (2019) 071103 [[1906.10840](#)].
- [17] R. Li and J. Wang, *Thermodynamics and kinetics of hawking-page phase transition*, *Phys. Rev. D* **102** (2020) 024085.
- [18] R. Li, K. Zhang and J. Wang, *Thermal dynamic phase transition of Reissner-Nordström Anti-de Sitter black holes on free energy landscape*, *JHEP* **10** (2020) 090 [[2008.00495](#)].
- [19] M. Fierz and W. Pauli, *On relativistic wave equations for particles of arbitrary spin in an electromagnetic field*, *Proc. Roy. Soc. Lond. A* **173** (1939) 211.
- [20] D. G. Boulware and S. Deser, *Can gravitation have a finite range?*, *Phys. Rev. D* **6** (1972) 3368.
- [21] C. de Rham, G. Gabadadze and A. J. Tolley, *Resummation of massive gravity*, *Phys. Rev. Lett.* **106** (2011) 231101.
- [22] R.-G. Cai, Y.-P. Hu, Q.-Y. Pan and Y.-L. Zhang, *Thermodynamics of Black Holes in Massive Gravity*, *Phys. Rev. D* **91** (2015) 024032 [[1409.2369](#)].
- [23] S. H. Hendi, R. B. Mann, S. Panahiyan and B. Eslam Panah, *Van der Waals like behavior of topological AdS black holes in massive gravity*, *Phys. Rev. D* **95** (2017) 021501 [[1702.00432](#)].
- [24] S. H. Hendi, B. Eslam Panah and S. Panahiyan, *Thermodynamical Structure of AdS Black Holes in Massive Gravity with Stringy Gauge-Gravity Corrections*, *Class. Quant. Grav.* **33** (2016) 235007 [[1510.00108](#)].
- [25] B. Mirza and Z. Sherkatghanad, *Phase transitions of hairy black holes in massive gravity and thermodynamic behavior of charged AdS black holes in an extended phase space*, *Phys. Rev. D* **90** (2014) 084006 [[1409.6839](#)].
- [26] S. Fernando, *Phase transitions of black holes in massive gravity*, *Mod. Phys. Lett. A* **31**

- (2016) 1650096 [[1605.04860](#)].
- [27] S.-L. Ning and W.-B. Liu, *Black Hole Phase Transition in Massive Gravity*, *Int. J. Theor. Phys.* **55** (2016) 3251.
  - [28] D.-C. Zou, R. Yue and M. Zhang, *Reentrant phase transitions of higher-dimensional AdS black holes in dRGT massive gravity*, *Eur. Phys. J. C* **77** (2017) 256 [[1612.08056](#)].
  - [29] B. Liu, Z.-Y. Yang and R.-H. Yue, *Tricritical point and solid/liquid/gas phase transition of higher dimensional AdS black hole in massive gravity*, *Annals Phys.* **412** (2020) 168023 [[1810.07885](#)].
  - [30] S. H. Hendi, B. Eslam Panah, S. Panahiyan, H. Liu and X. H. Meng, *Black holes in massive gravity as heat engines*, *Phys. Lett. B* **781** (2018) 40 [[1707.02231](#)].
  - [31] P. K. Yerra and C. Bhamidipati, *Critical heat engines in massive gravity*, *Class. Quant. Grav.* **37** (2020) 205020 [[2005.10115](#)].
  - [32] S.-Q. Lan, *Joule-Thomson expansion of neutral AdS black holes in massive gravity*, *Nucl. Phys. B* **948** (2019) 114787.
  - [33] M. Chabab, H. El Moumni, S. Iraoui and K. Masmar, *Phase transitions and geothermodynamics of black holes in dRGT massive gravity*, *Eur. Phys. J. C* **79** (2019) 342 [[1904.03532](#)].
  - [34] B. Wu, C. Wang, Z.-M. Xu and W.-L. Yang, *Ruppeiner geometry and thermodynamic phase transition of the black hole in massive gravity*, *Eur. Phys. J. C* **81** (2021) 626 [[2006.09021](#)].
  - [35] P. K. Yerra and C. Bhamidipati, *Ruppeiner Geometry, Phase Transitions and Microstructures of Black Holes in Massive Gravity*, *Int. J. Mod. Phys. A* **35** (2020) 2050120 [[2006.07775](#)].
  - [36] T. K. Safir, C. L. A. Rizwan and D. Vaid, *Ruppeiner geometry,  $P - V$  criticality and interacting microstructures of black holes in dRGT massive gravity*, *Int. J. Mod. Phys. A* **37** (2022) 2250158.
  - [37] D. Vegh, *Holography without translational symmetry*, [1301.0537](#).
  - [38] S. H. Hendi, R. B. Mann, S. Panahiyan and B. Eslam Panah, *Van der waals like behavior of topological ads black holes in massive gravity*, *Phys. Rev. D* **95** (2017) 021501.
  - [39] D. Kastor, S. Ray and J. Traschen, *Enthalpy and the Mechanics of AdS Black Holes*, *Class. Quant. Grav.* **26** (2009) 195011 [[0904.2765](#)].
  - [40] B. P. Dolan, *The cosmological constant and the black hole equation of state*, *Class. Quant.*

*Grav.* **28** (2011) 125020 [[1008.5023](#)].

- [41] B. P. Dolan, *Pressure and volume in the first law of black hole thermodynamics*, *Class. Quant. Grav.* **28** (2011) 235017 [[1106.6260](#)].